Coarsening kinetics in finite clusters

V. E. Fradkov, M. E. Glicksman, and S. P. Marsh*
Rensselaer Polytechnic Institute, Materials Engineering Department, Troy, New York 12180-3590
(Received 30 October 1995)

We address the problem of diffusional interactions in a finite sized cluster of spherical particles for volume fractions V_V, in the range 0–0.01. We determined the quasistatic monopole diffusion solution for n particles distributed at random in a continuous matrix. A global mass conservation condition is employed, obviating the need for any external boundary condition. The numerical results provide the instantaneous (snapshot) growth or shrinkage rate of each particle, precluding the need for extensive time-dependent computations. The close connection between these snapshot results and the coarse-grained kinetic constants are discussed. A square-root dependence of the deviations of the rate constants from their zero volume fraction value is found for the higher V_V investigated. The behavior is consistent with predictions from the diffusion Debye-Hückel screening theory. By contrast, a cube-root dependence, reported in earlier numerical studies, is found for the lower V_V investigated. The roll-over region of the volume fraction where the two asymptotics merge depends on the number of particles n alone. A theoretical estimate for the roll-over point predicts that the corresponding V_V varies as n^{-2}, in good agreement with the numerical results.

PACS number(s): 82.20.Wt, 81.40.Cd, 81.30.−t, 64.75.+g

I. INTRODUCTION

Diffusional coarsening represents an important and commonly observed kinetic process in microstructural evolution. Coarsening can occur among several microstructural constituents ranging from the primary phases to widely dispersed precipitates. The wide range of volume fractions V_V encountered in phase coarsening makes it essential to have a fundamental theory of coarsening that treats the volume fraction as an input parameter of the microstructure. The classical coarsening theory developed by Todes [1] and Lifshitz and Slyozov [2] (TLS theory) is limited to infinitesimally small volume fractions. To date, scores of papers have been published attempting to extend TLS theory to finite volume fractions intrinsic to real microstructures. Several excellent reviews have been published surveying these models along with relevant experiments [3–5]. Nonetheless, even finding the initial corrections to TLS theory in the limit of small volume fractions remains an open question. Specifically, the analytical theory for *infinite* systems suggested by Marqusee and Ross [6] and Marqusee [7], based on the diffusion analog of the Debye-Hückel screening effect, leads to deviations from TLS in the coarsening rate, which are proportional to $V_V^{1/2}$. By contrast, several numerical analyses [8,9] dealing with *finite* systems clearly show that this deviation is, instead, proportional to $V_V^{1/3}$. The purpose of the present paper is to analyze how the coarsening rates change in a finite cluster of a specified particle density. We will show numerically that both $V_V^{1/2}$ and $V_V^{1/3}$ behaviors may occur, depending on the number of particles comprising the cluster and its volume fraction. The crossover between these behaviors will be derived analytically using the Debye-Hückel screening concept.

II. THEORETICAL BACKGROUND: MEAN-FIELD APPROACHES

The simplest model of coarsening in infinitesimally sparse systems [1] assumes that all precipitate particles remain spherical and remote from each other, and that their positions remain stationary. The description of isothermal coarsening is given in [1] in terms of the radius distribution function $F(R,t)$, where R and t are the particle radius and the time. The norm of $F(R,t)$ is based on the total number of particles per unit volume N_V, that is,

$$\int_0^\infty F(R,t)dR = N_V \ . \tag{1}$$

With this normalization, the volume fraction V_V of the dispersed phase is given by

$$V_V \equiv \int_0^\infty F(R,t)\frac{4\pi}{3}R^3 dR = \frac{4\pi}{3}N_V\langle R^3\rangle \ . \tag{2}$$

Supersaturation of the matrix solution is assumed to be small, so that nucleation of new particles is precluded. The continuity equation for particles in size space is

$$\frac{\partial F}{\partial t}+\frac{\partial}{\partial R}[v(R)F]=0 \ , \tag{3}$$

where $v(R)$ is the time-rate of change of the radius R of a particle. To obtain $v(R)$, further simplifying assumptions were made: (a) the kinetics of coarsening is limited by volume diffusion; and (b) the diffusion is quasistatic. Therefore, the diffusion equation describing the concentration field, $c(\mathbf{r})$, in the matrix phase reduces to the Laplace equation

*Present address: Naval Research Laboratory, Physical Metallurgy Branch, Washington, D.C. 20375.

$$\nabla^2\varphi=0 , \tag{4}$$

where $\varphi=(c-c_0)/c_0$ and c_0 is the equilibrium solubility. The boundary conditions at the surface of the ith particle are specified through the Gibbs-Thomson local equilibrium relation

$$\varphi_i=\frac{\lambda}{R_i} , \tag{5}$$

where λ is the capillary length given by

$$\lambda=\frac{2\gamma\Omega}{k_B T} . \tag{6}$$

Here, γ is the particle-matrix specific interfacial energy, Ω is the atomic volume of the dispersed phase, k_B is the Boltzmann constant, and T is temperature. Additionally, anisotropy of the interfacial energy and strain effects were ignored.

The solution to Eq. (4), subject to the boundary conditions (5) at the interface of each particle, may be written in the form of the Coulomb potential (the solution given by Eq. (7) is a monopole approximation, where the particles are treated as point sources and sinks. This is justified by the large distances between the particles compared to their radii)

$$\varphi(\mathbf{r})=\sum_i \frac{\lambda B_i}{|\mathbf{r}-\mathbf{r}_i|}+\varphi_\infty , \tag{7}$$

where φ_∞ is the background-matrix diffusion potential, assumed uniform throughout the matrix phase; $\mathbf{r}$ is a field point always in the matrix; $\mathbf{r}_i$ locates the center of the ith particle. The diffusion analog of electrostatic charge is the volume flux per steradian, B_i, given by

$$B_i=\left[1-\frac{R_i}{R^*}\right] , \tag{8}$$

where the critical radius R^* is given by

$$R^*=\frac{\lambda}{\varphi_\infty} . \tag{9}$$

The time-rate of change of the radius, $v(R)$, used in Eq. (3), is directly connected to B_i as

$$v(R_i)=-\frac{2\lambda D c_0\Omega}{R_i^2}B_i . \tag{10}$$

Equation (8) provides the values of B_i, but the value of φ_∞ remains unknown. Todes suggested using the global conservation of volume of the dispersed phase, neglecting changes in the supersaturation within the matrix phase [1]:

$$\frac{d}{dt}\int_0^\infty F(R,t)\frac{4\pi}{3}R^3 dR\equiv\int_0^\infty\frac{\partial}{\partial t}F(R,t)\frac{4\pi}{3}R^3 dR=0 . \tag{11}$$

Using the continuity equation to substitute for $\partial F/\partial t$, one obtains

$$\varphi_\infty=\frac{\int_0^\infty F(R,t)dR}{\int_0^\infty F(R,t)RdR}\equiv\frac{1}{\langle R\rangle} , \text{ or } R^*=\langle R\rangle . \tag{12}$$

Todes also introduced a dimensionless variable $\rho=R/R^*$. The dimensionality of the diffusion-limited coarsening process implies that

$$R^*=\alpha(2\lambda D c_0\Omega t)^{1/3} , \tag{13}$$

where α is a dimensionless kinetic coefficient to be defined later. Todes then found a one-parameter family of self-similar solutions for the distribution function $F(R,t)$, given by the product-function form

$$F(R,t)=\frac{N_V(t)}{R^*(t)}f(\rho,\alpha) . \tag{14}$$

With Eq. (14), the continuity equation (3) reduces to the following ordinary differential equation:

$$\frac{df}{f}=\frac{-4\rho^3+(6/\alpha^3)(1-\rho)}{(3/\alpha^3)(1-\rho)+\rho^3}\frac{d\rho}{\rho} . \tag{15}$$

The number of real roots of the denominator, $\mathcal{D}=(3/\alpha^3)(1-\rho)+\rho^3$, on the right-hand side (rhs) of Eq. (15) depends on the value of α, which in turn influences the qualitative behavior of the solution to Eq. (15). Figures 1(a)–(c) show the three possible behaviors of the denominator. For $\alpha>(\frac{2}{3})^{2/3}$, Fig. 1(a), there is no real root of the denominator, and the solution to Eq. (15) is analytic up to infinity. This solution, however, causes a logarithmic divergency of the integral for the total volume of the particles. Truncating the logarithmic tail, however, destroys the self-similarity of the distribution function $f(\rho)$, because the relative density of particles at large ρ values is gradually exhausted. For $\alpha<(\frac{2}{3})^{2/3}$, Fig. 1(c), the solution must be restricted between zero and the first positive root of the denominator and set equal to zero beyond, in order to prevent singular behavior of the distribution function at the roots of the denominator. These solutions are, however, unstable with respect to appearance in the system of a particle outside of the permitted range as a result of coalescence. Lifshitz and Slyozov [2], therefore, stated that the only stable solution to the continuity equation (3) corresponds to such a value of α that makes the two positive roots of the denominator coincide, Fig. 1(b). That implies

$$\alpha_{\mathrm{TLS}}=(2/3)^{2/3} . \tag{16}$$

It is important to note that although the TLS solution to coarsening kinetics does not depend formally on the value of the volume fraction V_V, *it is not,* in fact, *extensible to any nonzero volume fraction.* The restriction of the TLS solution to the zero volume fraction is a consequence of the contradiction between the infinite extent of the Laplace diffusion field and the total neglect of direct interactions among the particles. This contradiction manifests itself even stronger in two dimensions, where an analogous TLS theory cannot even be developed without imposing some arbitrary cutoff radius to the diffusion field, due to its logarithmic far-field behavior for each individual particle [8,9].

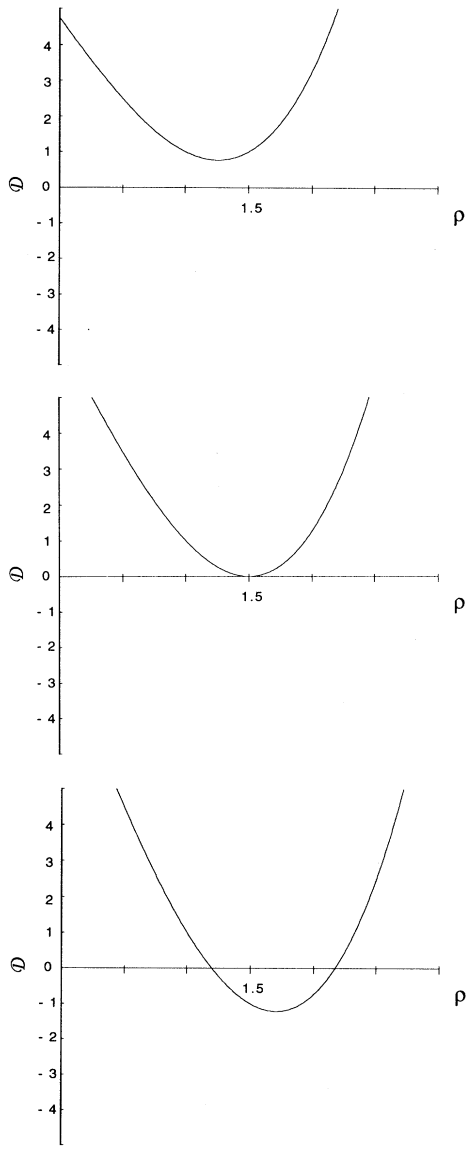

FIG. 1. Behavior of the denominator $\mathcal{D}$ of Eq. (15): (a) $\alpha > (\frac{2}{3})^{2/3}$, (b) $\alpha = (\frac{2}{3})^{2/3}$, (c) $\alpha < (\frac{2}{3})^{2/3}$.

There are two general approaches that are used to incorporate the influence of the volume fraction on coarsening kinetics. The earliest approaches were based on arbitrary restriction of the extent of the interparticle diffusional interactions to the average interparticle separation (see [17] for a review). In sparse systems the nearest neighbors, of course, cannot shield the Laplacian field. Theories based on models using interparticle distance for the cutoff are generally in poor agreement with experiment and numerical simulations [3,4,17]. For higher volume fractions, $0.1 < V_V < 0.6$, however, direct screening by nearest neighbors becomes more reasonable, but generally the models that use a single cutoff radius do not provide meaningful results for the specified range of volume fractions (see Ref. [10] for a review).

Marqusee and Ross [6] and Marqusee [7], by contrast, restricted the extent of the Laplacian diffusion field by taking into account screening effects in active two-phase media containing a distribution of diffusional sources and sinks. Instead of the Laplace equation, Marqusee and Ross obtained the Poisson equation for the spatially coarse-grained background diffusion potential φ, namely,

$$\nabla^2\varphi = -4\pi\sigma \ , \tag{17}$$

in which the source/sink density σ, in the matrix space surrounding a particle is given by

$$\sigma(\mathbf{r}) = \int_0^\infty \lambda B F(R,t)dR = \int_0^\infty [\lambda - R\varphi(\mathbf{r})]F(R,t)dR \ . \tag{18}$$

Note that here the background potential in Eq. (8), φ_∞, is replaced by the coarse-grained potential φ, which is consistent with Debye's approach. Carrying out the indicated integration on the right-hand side of Eq. (18) gives

$$\sigma(\mathbf{r}) = N_V\lambda - N_V\langle R\rangle\varphi(\mathbf{r}) \ , \tag{19}$$

where N_V and $\langle R\rangle$ are defined by Eqs. (1) and (12), respectively. Substituting Eq. (19) into Eq. (17) yields the diffusion analog of the Debye-Hückel equation, namely,

$$\nabla^2\varphi - \kappa^2(\varphi - \varphi_\infty) = 0 \ , \tag{20}$$

where

$$\kappa^2 = 4\pi N_V\langle R\rangle \tag{21}$$

and

$$\varphi_\infty = \lambda/\langle R\rangle \ . \tag{22}$$

Equation (20) is well known from the theories of ionic plasmas and electrolytes, where it is used to describe the electrostatic field developed in an active medium containing a distribution of quantized charges. In these theories, the second term on the left-hand side of Eq. (20) describes the space charge density caused by spatial redistribution of the charges, in order to minimize the electrostatic energy. In the case of diffusional coarsening, however, the positions of the "charges" (diffusional source/sink strengths) are fixed, but their values, the B_i's, depend on the *local* background potential $\varphi(\mathbf{r})$, consistent with Eq. (8).

The solution to Eq. (20) subject to the boundary conditions, Eq. (5), is in the form of a Yukawa potential,

$$\varphi(\mathbf{r}) = \sum_i \frac{\lambda B_i}{|\mathbf{r}-\mathbf{r}_i|}\exp(-\kappa|\mathbf{r}-\mathbf{r}_i|) + \varphi_\infty \ , \tag{23}$$

where now the B_i's are defined as

$$B_i = \left[1 - \frac{R_i\varphi_\infty}{\lambda}\right](1+\kappa R_i) = B_i^{\mathrm{TLS}}(1+\kappa R_i) \ . \tag{24}$$

B_i^{TLS} denotes the dimensionless volume fluxes (per steradian) for particles in an infinitesimally dilute system, as given in the TLS theory by Eq. (8). The coefficient κ is the reciprocal of the diffusional analog of the Debye screening length. It represents the natural cut-off distance for direct particle interactions via the diffusion

field, beyond which the particles are isolated from each other by the intervening two-phase medium. As seen from Eq. (24), κR_i expressly captures the deviations in the rate of particle size evolution from the TLS limit. It is possible to use the same global stability analysis introduced by Lifshitz and Slyozov [2] to obtain the characteristic kinetic constant α, which determines the overall rate of coarsening as defined in Eq. (13) (see [6] for details):

$$\alpha(V_V)=\alpha_{\mathrm{TLS}}(1+0.740V_V^{1/2}+\text{h.o.t.}) , \tag{25}$$

where $\alpha_{\mathrm{TLS}}=(\frac{2}{3})^{2/3}$ is the TLS limit for infinitesimally diluted systems ($V_V=0$). Equation (25) shows that the average particle size grows more rapidly than in the TLS limit. Moreover, this correction, reflecting diffusional Debye screening, implies other first-order corrections, including the broadening of the size distribution function and the difference between the average and the critical radii; all these corrections are proportional to the square root of the volume fraction.

III. KINETIC PROPERTIES OF FINITE COARSENING SYSTEMS

There are four physically distinct metric scales in any *finite* coarsening cluster, i.e., a finite number of particles confined to a finite volume: (i) the size of the particles, as characterized by $\Lambda_R \approx \langle R \rangle$; (ii) the interparticle spacing, as characterized by $\Lambda_N \approx N_V^{-1/3}$, where N_V is the total number of particles per unit volume, Eq. (1); (iii) the Debye screening radius $\Lambda_D \equiv \kappa^{-1}$; and (iv) the extent of the total coarsening system Λ_{tot}, as defined for a "spherical cluster" by $\Lambda_{\mathrm{tot}}=(4\pi/3)^{-1/3}(n/N_V)^{1/3}$, where n is the total number of particles remaining at a given time. Note, it is always assumed that the cluster is locally homogeneous and spatially isotropic, and that the overall size of the cluster, Λ_{tot}, is time independent. These assumptions permit one to establish an analog of the volume fraction for a finite cluster of particles,

$$V_V=\frac{\sum_{i=1}^{n}\frac{4\pi}{3}R_i^3}{\frac{4\pi}{3}\Lambda_{\mathrm{tot}}^3} , \tag{26}$$

where the denominator in Eq. (26) provides an estimate of the spherical cluster volume.

By contrast with infinite systems, finite systems lack *uniform* asymptotics, because any finite system ultimately achieves its end state as a single particle in finite time. Finite systems, instead, may only exhibit *intermediate* asymptotics. By this we mean that the coarse-grained average over time of these cluster parameters becomes identical to those in self-similar infinite systems, even though the instantaneous values of the time-dependent parameters of finite clusters may fluctuate. All continuum coarsening theories, however, exclusively yield quantities that are equivalent to the coarse-grained averages over time for finite clusters. Specifically, therefore, the coarse-grained *intensive* length scale parameters, viz. Λ_N, Λ_R, and Λ_D, are expected to scale with time as predicted by continuum coarsening theories.

Weins and Cahn [11] were the first to estimate the diffusional interactions among a few particles comprising a small coarsening cluster. Later Voorhees and Glicksman [12,13] extended Weins and Cahn's analysis to hundreds of particles by using periodic boundary conditions, and adapted Ewald sums to improve the convergence of the numerical calculations. In finite systems, coarsening always occurs via two distinct but related processes: the *continuous* evolution of the particle radii, and the *discontinuous* (instantaneous) disappearance of the smallest particles. The coarse-grained time averages depend on both processes. Specifically, during the continuous process, the average size of the particles decreases (along with the total interfacial area), whereas the instantaneous disappearances cause the average size to increase. The actual evolution of the average radius consists of smoothly falling segments connected by vertical jumps whenever a particle disappears, as observed in computer simulations [13,15]. The coarse-grained average changed with time as $t^{1/3}$, according to the TLS prediction.

A recent simulation and experimental study of coarsening in finite clusters of three-dimensional particles interacting through a two-dimensional diffusion field [14,15] shows similar discontinuous behavior of the average radius, whereas the coarse-graining behavior of the average particle radius exhibited a power law of $t^{1/4}$, characteristic of the continuum coarsening prediction for the mixed-dimensional case (see Fig. 2). Thus, experiments confirm and simulations show that the coarse-grained intermediate asymptotic behavior of real, i.e., finite, coarsening systems is consistent with theoretically predicted asymptotic power laws from continuum theories.

Normally, the numerical data required for coarse-grained averaging are obtained by time-dependent computer simulations. Following such procedures for large clusters (tens of thousands of particles) is computationally intensive. There would be a great advantage in large

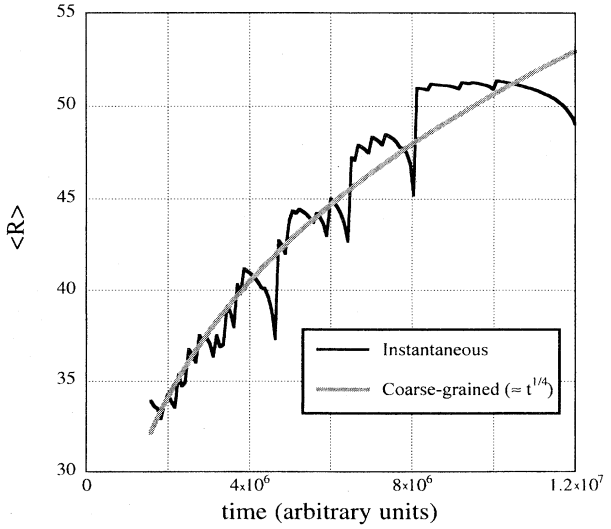

FIG. 2. Instantaneous and coarse-grained time dependence of the average particle size observed in computer simulation of mixed-dimensional cluster coarsening [14,15].

finite systems to limiting the numerical simulation to a "snapshot" analysis of the rate of change of $\langle R \rangle$ along the continuous segments. It is unclear, however, how the instantaneous slopes $v(R_i)$, defined by Eq. (10), are related to the coarse-grained average time dependence of $\langle R \rangle$. One can show, using first-order perturbation theory, that the relative change in the kinetic constant, α, from the Lifshitz-Slyozov stability analysis is proportional to the relative change in the growth rate $v(R_{\max})$, for the largest particle within the TLS distribution, induced by any small perturbation. Specifically, if a small disturbance to the particle growth rates, $\varepsilon(R)$, is introduced as

$$v(R)=v_{\rm TLS}(R)[1+\varepsilon(R)] , \tag{27}$$

where $v_{\rm TLS}$ is the nonperturbed value given by the TLS theory, Eq. (10). The denominator, $\mathcal{D}$, in Eq. (15), becomes

$$\mathcal{D}=\rho^3-\beta(\rho-1)(1+\varepsilon) , \tag{28}$$

where $\beta=3/\alpha^3$. Following the procedure set out in Sec. II, we find the eigenvalue for β and the maximum value of ρ by solving the equation set $\mathcal{D}=0$ and $\mathcal{D}'=0$. Seeking first-order corrections to the eigenvalue, we write

$$\beta=\beta_{\rm TLS}+\delta\beta \tag{29}$$

and

$$\rho=\rho_{\rm TLS}+\delta\rho , \tag{30}$$

where $\rho_{\rm TLS}=\frac{3}{2}$, and $\beta_{\rm TLS}=\frac{27}{4}$. Keeping only first-order terms, we find

$$\mathcal{D}=-\delta\beta/2-(27/8)\varepsilon=0 , \tag{31}$$

where ε is evaluated at $\rho_{\rm TLS}=\frac{3}{2}$. This results in $\delta\eta=-(\frac{27}{4})\varepsilon$, and

$$\alpha=\alpha_{\rm TLS}[1+(3/16)^{1/3}\varepsilon(R^{\rm TLS}_{\max})] . \tag{32}$$

Here, $R^{\rm TLS}_{\max}=(\frac{3}{2})\langle R \rangle$ and $\alpha_{\rm TLS}=(\frac{2}{3})^{2/3}$ are the nonperturbed values given by the TLS theory. For example, if the perturbation $\varepsilon(R)$ is caused by diffusional Debye screening, Eq. (24), then Eq. (32) transforms to Eq. (25) from the analysis by Marqusee and Ross [7]. The second equation, $\mathcal{D}'=0$, may be written as $\partial\mathcal{D}/\partial\delta\rho=0$, or, keeping first-order terms,

$$\mathcal{D}'=6\rho_{\rm TLS}\delta\rho-\delta\beta-\beta_{\rm TLS}\varepsilon-\beta_{\rm TLS}(\rho_{\rm TLS}-1)\varepsilon'=0 . \tag{33}$$

This gives the correction in $\rho_{\max}$, which, however, depends not on ε but on $\varepsilon'=\partial\varepsilon/\partial\delta\rho$,

$$\delta\rho=(3/8)\varepsilon' . \tag{34}$$

The snapshot numerical analysis, to be discussed below, is capable of providing the $\varepsilon(R)$ values for each particle in the cluster. In a finite cluster, however, one does not have a statically valid representation of enough particles at $R_{\max}$ to guarantee an accurate estimate of $\varepsilon(R_{\max})$. Consequently, we will *average the perturbations over the entire system of particles, using the assumption that the global average, $\langle \varepsilon(R) \rangle$, reflects the behavior of* $\varepsilon(R_{\max})$. This assumption is a rather likely outcome of the self-similar behavior we are discussing.

IV. "SNAPSHOT" NUMERICAL ANALYSIS

The mathematical formulation for the present numerical study is based on the monopole approximation to the quasistatic diffusion solution shown in Eq. (7). The particle growth rates were calculated for each individual particle in the cluster according to Eq. (7), using the exact monopole expressions for the dimensionless diffusional source/sink strengths B_i's, namely,

$$B_i=\left[1-\frac{R_i}{\lambda}\left[\varphi_\infty+\sum_{j=1,j\neq i}^{n}\frac{B_j}{|\mathbf{r}_j-\mathbf{r}_i|}\right]\right] . \tag{35}$$

Here n is the total number of particles in the cluster, λ is a capillary length defined in Eq. (6), and the expression in the parenthesis represents the local analog of the background diffusion potential used in the TLS theory, Eq. (8). Equation (35) represents a set of n linear equations with $n+1$ unknowns, viz., the B_i's and φ_∞. One additional equation is needed to close the system. In previous simulations such an equation was provided by an external boundary condition, e.g., the periodicity condition used in [9,13]. In the present work we employ, instead, a conservation equation for the total volume of the particles, as suggested in [11,15]:

$$\sum_{i=1}^{n} B_i=0 . \tag{36}$$

A version of the Gauss-Seidel iterative algorithm was employed for solving the set of equations given by Eqs. (35) and (36), which equations may be written in matricial form as

$$\begin{bmatrix}
\frac{\lambda}{R_1} & \frac{\lambda}{|\mathbf{r}_1-\mathbf{r}_2|} & \frac{\lambda}{|\mathbf{r}_1-\mathbf{r}_3|} & \cdots & 1 \\
\frac{\lambda}{|\mathbf{r}_1-\mathbf{r}_2|} & \frac{\lambda}{R_2} & \frac{\lambda}{|\mathbf{r}_2-\mathbf{r}_3|} & \cdots & 1 \\
\frac{\lambda}{|\mathbf{r}_3-\mathbf{r}_1|} & \frac{\lambda}{|\mathbf{r}_3-\mathbf{r}_2|} & \frac{\lambda}{R_3} & \cdots & 1 \\
\cdot & \cdot & \cdot & \cdots & 1 \\
\cdot & \cdot & \cdot & \cdots & 1 \\
\cdot & \cdot & \cdot & \cdots & 1 \\
1 & 1 & 1 & 1\ 1\ 1\ 0 &
\end{bmatrix}
\begin{bmatrix} B_1 \\ B_2 \\ B_3 \\ \cdot \\ \cdot \\ \cdot \\ \varphi_\infty \end{bmatrix}
=
\begin{bmatrix} \frac{\lambda}{R_1} \\ \frac{\lambda}{R_2} \\ \frac{\lambda}{R_3} \\ \cdot \\ \cdot \\ \cdot \\ 0 \end{bmatrix} . \tag{37}$$

A linear projection to $n \times n$ subspace was employed to eliminate the last row and column and make the matrix, Eq. (37), suitable for applying the classical Gauss-Seidel linear solver.

The cluster parameters in the "snapshot" simulation are the set of n particle center coordinates $\{\mathbf{r}_i\}$ and the set of n particle radii $\{R_i\}$, both of which are measured in units of λ. The n particle center coordinates in this simulation are chosen randomly inside a sphere of radius $\Lambda_{\rm tot}$. Each particle was assigned a radius randomly distributed around the average value $\langle R \rangle = \Lambda_R$ according to various distributions. Specifically, we used the TLS particle-size distribution and rectangular distributions of various widths. An influence of the particle-size distribution on the kinetic results was not observed. The particles are not allowed to overlap. This restriction results in some correlation between particle sizes and positions, which tends to vanish with decreasing volume fraction. The volume fraction itself was varied by changing the ratio $\Lambda_R^3/\Lambda_{\rm tot}^3$, according to Eq. (26), while maintaining fixed relative positions and radii of the particles. Specifically, we proportionally changed all the interparticle distances and, consequently, changed the size of the cluster and the volume fraction, whereas the particle radii remained constant.

V. RESULTS AND DISCUSSION

Figure 3 shows the dependence of the volume fraction of the observed relative deviations,

$$\Delta(V_V)=\frac{\langle \nu(R,V_V)\rangle-\langle \nu(R,0)\rangle}{\langle \nu(R,0)\rangle}\ , \tag{38}$$

in the values of the rate of change of the average radius $\langle \nu(R,V_V)\rangle$ compared to that for the zero volume fraction $\langle \nu(R,0)\rangle$. The values at nonzero volume fractions were obtained from the snapshot calculations, using Eq. (37), whereas the zero volume fraction term is obtained from the TLS expression, Eq. (8). The results are shown for clusters containing 10, 100, and 1000 particles. The deviations are plotted on log-log coordinates vs the volume fraction V_V, given by Eq. (26), which was varied for each calculation by changing the ratio $\Lambda_R^3/\Lambda_{\rm tot}^3$, as described above. There appear to be two distinguished limits for the slopes, representing the exponents of the leading-order corrections introduced by the volume fraction. For the higher ranges of volume fraction the exponent is $\frac{1}{2}$, in agreement with Debye screening theory, Eq. (24). Combining Eqs. (2), (8), (10), (21), and (24) with the definition of Δ, Eq. (38), we obtain the expression for Δ in terms of the volume fraction,

$$\Delta=\left[\frac{1-\mu_{-1}}{\mu_{-1}-\mu_{-2}}\right]\left[\frac{3}{\mu_3}\right]^{1/2}V_V^{1/2}=0.695V_V^{1/2}\ , \tag{39}$$

where the μ_i's are the ith moments of the TLS distribution defined as

$$\mu_i=\frac{\int_0^\infty R^i F(R,t)dR}{\langle R\rangle^i N_V}\ . \tag{40}$$

The coefficient on the rhs of Eq. (39) is slightly different from that appearing in Eq. (25), because these coefficients reflect different combinations of the moments of the distribution function.

For the lower ranges of volume fraction the exponent appearing in Fig. 3 is $\frac{1}{3}$, consistent with earlier simulations [13] and theories employing a cut-off radius based

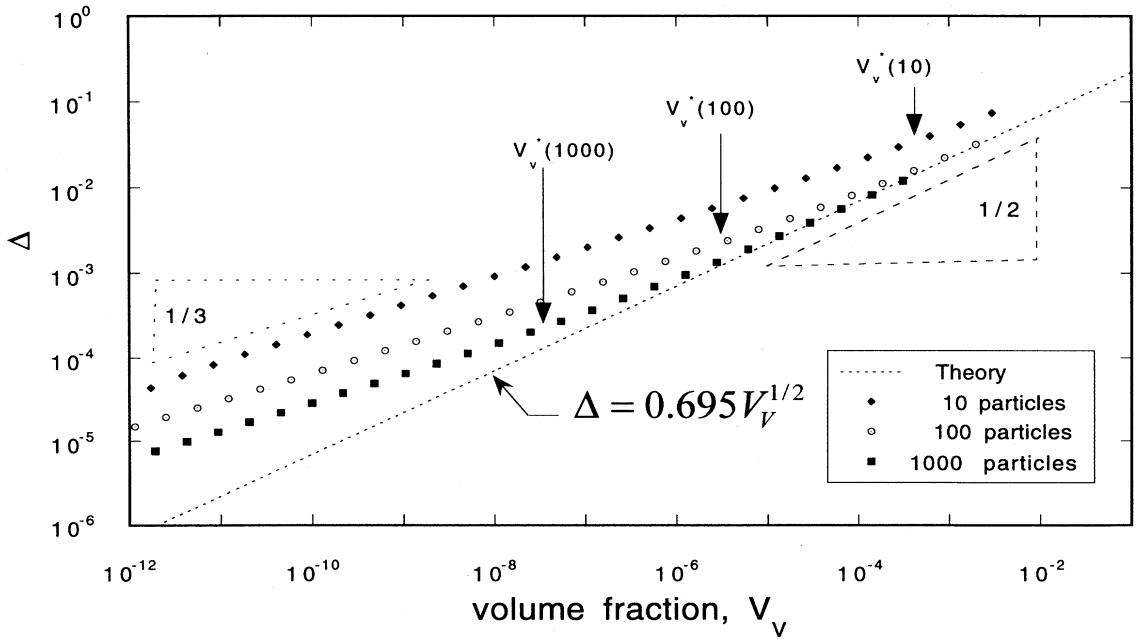

FIG. 3. Relative deviation Δ of the kinetic rate constant for the coarsening of finite clusters at various volume fractions from that at zero volume fraction. These data are obtained by snapshot monopole calculations. The theory refers to Eq. (39). Arrows correspond to the rollover volume fractions, where the exponent changes from $\frac{1}{3}$ to $\frac{1}{2}$, as predicted by Eq. (45).

on the interparticle separation [16]. The roll-over point between the two exponents depends on the number of particles, n, in the cluster, so that for clusters with larger n the transition occurs at progressively lower volume fractions. To explain the observed rollover behavior we substitute Eq. (2) into Eq. (21). This yields the Debye screening length Λ_D in terms of volume fraction V_V as

$$\Lambda_D = 3^{-1/2}(\langle R^3\rangle/\langle R\rangle)^{1/2}(V_V)^{-1/2} . \tag{41}$$

The spatial extent of the cluster, $\Lambda_{\rm tot}$, can also be estimated in terms of V_V as

$$\Lambda_{\rm tot} = (4\pi/3)^{-1/3}(n/N_V)^{1/3} = n^{1/3}\langle R^3\rangle^{1/3}(V_V)^{-1/3} . \tag{42}$$

A comparison of Eqs. (41) and (42) shows that the Debye screening distance grows faster with decreasing volume fraction than does the cluster size, holding other system parameters constant. This implies that at some small volume fraction, V_V^*, the Debye screening distance Λ_D exceeds the cluster size, and then diffusional screening is precluded.

When screening is no longer possible because of the sparsity of the cluster, then the deviations from TLS theory no longer have to be proportional to $V_V^{1/2}$. Indeed, comparing the TLS result, Eq. (8), with the monopole expression, Eq. (35), one obtains for the deviation from TLS

$$\delta B_i = \left[-\frac{R_i}{\lambda} \left[\sum_{j=1, j\neq i}^{n} \frac{B_j + \delta B_j}{|\mathbf{r}_j - \mathbf{r}_i|} \right] \right] . \tag{43}$$

For a sparse system, δB_j on the rhs of Eq. (43) may be neglected. The rhs of Eq. (43) may then be estimated, using the fundamental metric scales of the system, as $B_i \Lambda_R / \Lambda_N$. In terms of the volume fraction, one may express Eq. (35) as

$$\frac{\delta B_i}{B_i} \approx -\frac{\Lambda_R}{\Lambda_N} \approx \frac{\langle R\rangle}{N^{-1/3}} = \frac{\langle R\rangle}{\langle R^3\rangle^{1/3}} V_V^{1/3} . \tag{44}$$

Equation (44) shows that for extremely sparse clusters, the leading order deviation from TLS kinetics goes as $V_V^{1/3}$. This result is consistent with the asymptotic analysis performed in [12] for a periodic system.

The rollover point at which the exponent changes from $\frac{1}{2}$ to $\frac{1}{3}$ occurs when the Debye screening distance becomes comparable to the cluster size. The corresponding volume fraction, V_V^*, may be estimated from the condition $\Lambda_{\rm tot} = \Lambda_D$, which with the use of Eqs. (41) and (42) gives the result

$$V_V^* = \frac{\langle R^3\rangle}{\langle R\rangle^3} \frac{1}{27n^2} \approx \frac{1}{27n^2} . \tag{45}$$

Figure 3 also shows the theoretical rollover points calculated from Eq. (45) denoted by vertical arrows for clusters containing $n = 10$, 100, and 1000 particles. The predictions from Eq. (45) appear satisfactory for $n = 100$ and 1000, despite the fact that the clusters investigated here have relatively few particles to provide the Debye screening behavior. We note that a cluster with 1000 particles contains only about six interparticle distances from its center to its periphery. The cluster containing ten particles fails to show screening behavior for volume fractions approaching 1%. Diffusional interactions in clusters with volume fractions above about 1% would not be represented accurately by the monopole approximation.

VI. CONCLUSION

(i) Monopole snapshot calculations provide an efficient method for estimating the coarse-grained rate constants in finite clusters of coarsening particles. Prior to the development of this technique, fully time-dependent simulations were required to obtain this information.

(ii) Extending the definition of volume fraction to a finite cluster permits investigating the influence of the nonzero volume fraction on the coarsening kinetics.

(iii) The present results confirm that in finite clusters in the limit of low volume fraction the leading correction to the TLS rate constant is proportional to $V_V^{1/3}$. For higher volume fractions, or for a sufficient number of particles, Debye screening occurs and the leading-order term becomes proportional to $V_V^{1/2}$.

(iv) The rollover point between the two kinetic behaviors, that is, the critical volume fraction at which the Debye screening distance is comparable to the cluster size, is given by Eq. (45) and depends on the number of particles in the cluster. For clusters with only 1000 particles, the roll-over point is already as low as ca. 3×10^{-8}. This implies that in most experimental coarsening systems $V_V^{1/3}$ behavior should not occur.

(v) Inasmuch as Debye screening is not directly applicable to small clusters, its apparent success in explaining the results of these calculations requires further analysis. Larger-scale calculations with clusters containing much greater numbers of particles will be required to resolve this interesting issue, as well as to provide additional information on correlation effects and the influence of the cluster periphery on coarsening kinetics.

(vi) At volume fractions above ca. 1%, particle interactions become more complex than can be described with monopole approximations and Debye screening. Other techniques that incorporate spatial correlations among the particles, shape changes, direct screening, and higher-order multipole interactions must be employed.

ACKNOWLEDGMENTS

The authors gratefully acknowledge the support provided by the National Science Foundation, Division of Materials Research, Washington, DC, under Grant No. DMR93-07725, and the NASA Marshall Space Flight Center, Huntsville, AL, under Cooperative Agreement No. NCC8-54. The authors also acknowledge the contributions of Dr. V. Belsky concerning numerical algorithms, and Mr. M. Rutman, who assisted in carrying out the programming and the numerical calculations.

[1] O. M. Todes, J. Phys. Chem. **20**, 629 (1946).
[2] I. M. Lifshitz and V. V. Slyozov, J. Phys. Chem. Solids **19**, 35 (1961).
[3] P. W. Voorhees, J. Stat. Phys. **38**, 231 (1985).
[4] P. W. Voorhees, Ann. Rev. Mater. Sci. **22**, 197 (1992).
[5] Y. Enomoto, M. Tokuyama, and K. Kawasaki, Acta Metall. **35**, 907 (1987).
[6] J. A. Marqusee and J. Ross, J. Chem. Phys. **80**, 536 (1984).
[7] J. A. Marqusee, J. Chem. Phys. **81**, 976 (1984).
[8] B. K. Chakraverty, J. Phys. Chem. Solids **28**, 2401 (1967).
[9] S. P. Marsh, M. E. Glicksman, and D. B. Dadyburjor, J. Catalysis **99**, 358 (1986).
[10] Y. Enomoto, M. Tokuyama, and K. Kawasaki, Acta Metall. **34**, 2119 (1986).
[11] J. J. Weins and J. W. Cahn, *Sintering and Related Phenomena,* edited by G. C. Kuczynski (Plenum, London, 1973), p. 151.
[12] P. W. Voorhees and M. E. Glicksman, Acta Metall. **32**, 2001 (1984).
[13] P. W. Voorhees and M. E. Glicksman, Acta Metall. **32**, 2013 (1984).
[14] J. R. Rogers *et al.*, J. Electron. Mater. **23**, 841 (1994).
[15] V.E. Fradkov *et al.*, J. Electron. Mater. **23**, 849 (1994).
[16] S. P. Marsh, Ph.D. thesis, Rensselaer Polytechnic Institute, Troy, N.Y., 1989 (unpublished).
[17] K. Tsumuraya and Y. Miyata, Acta Metall. **31**, 437 (1983).